PREDICTING TEMPERATURE BEHAVIOR IN CARBONATE ACIDIZING TREATMENTS

A Thesis

by

XUEHAO TAN

Submitted to the Office of Graduate Studies of
Texas A&M University
in partial fulfillment of the requirements for the degree of

MASTER OF SCIENCE

May 2009

Major Subject: Petroleum Engineering

PREDICTING TEMPERATURE BEHAVIOR IN CARBONATE ACIDIZING TREATMENTS

A Thesis

by

XUEHAO TAN

Submitted to the Office of Graduate Studies of
Texas A&M University
in partial fulfillment of the requirements for the degree of

MASTER OF SCIENCE

Approved by:

Chair of Committee,	Ding Zhu
Committee Members,	A. Daniel Hill
	Sy-Bor Wen
Head of Department,	Stephen A. Holditch

May 2009

Major Subject: Petroleum Engineering

ABSTRACT

Predicting Temperature Behavior in Carbonate Acidizing Treatments. (May 2009)

Xuehao Tan, B.E., Tsinghua University

Chair of Advisory Committee: Dr. Ding Zhu

To increase the successful rate of acid stimulation, a method is required to diagnose the effectiveness of stimulation which will help us to improve stimulation design and decide whether future action, such as diversion, is needed.

For this purpose, it is important to know how much acid enters each layer in a multilayer carbonate formation and if the low-permeability layer is treated well.

This work develops a numerical model to determine the temperature behavior for both injection and flow-back situations. An important phenomenon in this process is the heat generated by reaction, affecting the temperature behavior significantly. The result of the thermal model showed significant temperature effects caused by reaction, providing a mechanism to quantitatively determine the acid flow profile. Based on this mechanism, a further inverse model can be developed to determine the acid distribution in each layer.

DEDICATION

This thesis is dedicated to my parents,

Fengke Tan and *Chao Jin*

ACKNOWLEDGEMENTS

I want to take this opportunity to thank my advisor and committee chair, Dr. Ding Zhu, for advice and help on my research. She always pointed out the right path for my research. I also want to thank Dr. A.D. Hill for his advice.

I want to thank another member of my committee, Dr. Sy-Bor Wen, for his patience and help.

I also appreciate the help from my colleagues, Weibo Sui, Jurairat Densirimongkol, Preston Fernandes, Manabu Nozaki, Maysam Pournik and Zhuoyi Li. I learned a lot from them.

I would like to thank my girlfriend, Jiajing Lin, for her patience and support.

Finally, I would like to acknowledge the financial support from the Middle East Carbonate Stimulation joint industry project at Texas A&M University. The facilities and resources provided by the Harold Vance Department of Petroleum Engineering in Texas A&M University are gratefully acknowledged.

TABLE OF CONTENTS

Page

ABSTRACT iii

DEDICATION iv

ACKNOWLEDGEMENTS v

TABLE OF CONTENTS vi

LIST OF FIGURES viii

LIST OF TABLES x

1. INTRODUCTION 1

    1.1 Problem Statement 1
    1.2 Status of Current Research 2
    1.3 Importance 4
    1.4 Objective and Procedures 4
    1.5 Outline 5

2. ACID INJECTION PROBLEM 6

    2.1 Introduction 6
    2.2 Energy Balance Equation 7
    2.3 Reaction between Acid and Rock 10
    2.4 Wormhole Growth Model 11
    2.5 Modified Volumetric Model 14
    2.6 Solution of Acid Injection Problem 15
    2.7 Validation of Injection Model 18
    2.8 Section Summary 19

3. FLOW-BACK PROBLEM 21

    3.1 Introduction 21
    3.2 Governing Equation 21
    3.3 Solution of Flow-Back Problem 22
    3.4 Section Summary 25

Page

4. RESULTS AND DISCUSSION 26

4.1 Introduction 26
4.2 Temperature Profile during Injection 26
4.3 Temperature Profile during Flowing Back 33
4.4 Sensitivity Study 36
4.5 Section Summary 40

5. CONCLUSIONS AND RECOMMENDATIONS 42

5.1 Conclusions 42
5.2 Recommendations and Future Work 42

NOMENCLATURE 44

REFERENCES 48

VITA 51

LIST OF FIGURES

FIGURE		Page
1.1	Multilayer carbonate reservoir has layers with different permeability	2
2.1	Wormhole front and spent acid front form and reaction occurs at wormhole front	7
2.2	Energy balance in the finite small element	8
2.3	Core flow test results. Pore volumes to breakthrough as a function of injection rate. (Buijse and Glasbergen 2005)	13
2.4	Flow chart for programming acid injection problem	17
2.5	Temperature in the formation for a constant injection temperature of 298 K (Medeiros and Trevisan 2006).....	18
2.6	Temperature simulated by our model for the same case	19
3.1	Flow chart for programming flow-back problem.....	24
4.1	Temperature distribution in the formation for q=1 bbl/min after injecting for 10 min	28
4.2	Temperature distribution in the formation for different injection rate after injecting for 10 min	28
4.3	Temperature distribution in the formation for different injection time when q=0.5 bbl/min.....	29
4.4	Temperature distribution in the formation for different injection time when q=1 bbl/min.....	30
4.5	Wormhole front and spent acid front when q= 1 bbl/min	31
4.6	Break through pore volumes as a function of time greater than 1 when q=1 bbl/min.....	31
4.7	Wormhole efficiency as a function of time when q=1 bbl/min	32

FIGURE Page

4.8 Average porosity of treated formation as a function of time when q=1 bbl/min..... 33

4.9 Temperature profile in the formation when the well is flowing back at 0.5 bbl/min after injection for 10 min (0.5bbl/min) 34

4.10 Temperature profile in the formation when the well is flowing back at 1 bbl/min after injection for 10 min (1 bbl/min) 34

4.11 Temperature profile in the formation when the well is flowing back at 1 bbl/min after injection for 20 min (1 bbl/min) 35

4.12 Temperature measured at the wellbore for different flow rate after 10 min injection 36

4.13 Comparison of injection temperature profile for different porosity..... 37

4.14 Comparison of wellbore temperature profile for different porosity..... 38

4.15 Comparison of injection temperature profile for different heat conductivity..... 39

4.16 Comparison of wellbore temperature profile for different heat conductivity..... 39

4.17 Comparison of wellbore temperature profile for different injection rate... 40

LIST OF TABLES

TABLE Page

2.1 Enthalpy of Reactants and Resultants (Perry et al. 1963) 11

4.1 Input Data 27

1. INTRODUCTION

1.1 Problem Statement

Acidizing treatments is one of the well stimulation technologies during which the acid is injected to the well. The acid reacts with rock and removes the damage in the near wellbore region. Hence, the production can be increased significantly, especially for carbonate reservoir, since the acid reacts faster with carbonate than sandstone.

For vertical wells in multilayer carbonate formation (**Fig. 1.1**), the layers with higher permeability accept most of the injected acid, which means the low-permeability layers are not treated as desired. The low permeability is not only caused by the natural structure of this layer, but also by the damage. In such a case, the acidizing job could be considered ineffective. To avoid inefficient treatments, a method is demanded to determine the amount of acid enters each layer to evaluate the acidizing treatments and to optimize acid treatment design.

To generate acid distribution in an acid stimulation, temperature measurement along the wellbore is possible today because of the development of downhole temperature sensor (DTS). The downhole temperature sensor provides continuous and accurate measurements.

This thesis follows the style of *SPE Journal*.

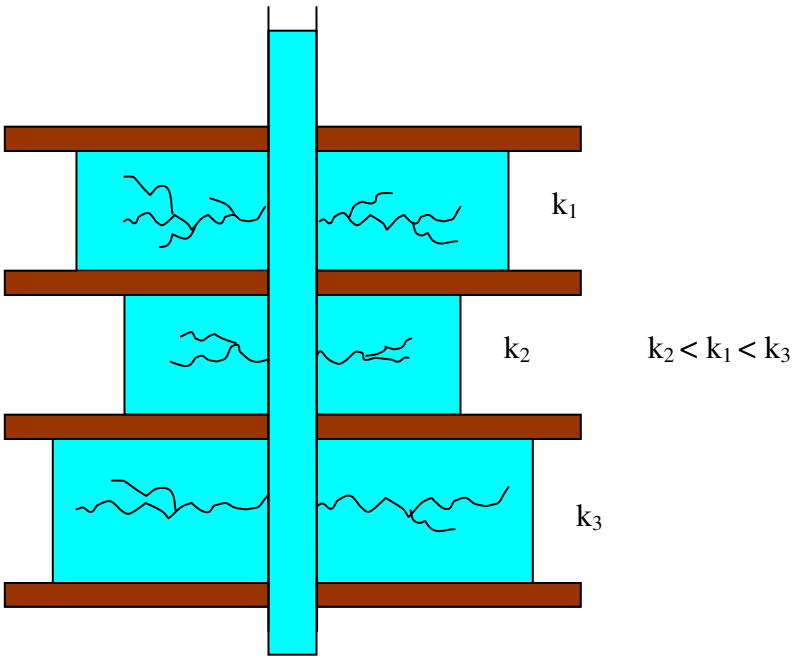

Fig. 1.1—Multilayer carbonate reservoir has layers with different permeability

1.2 Status of Current Research

Acidizing stimulation is a very important method to increase production in a carbonate reservoir. To ensure the efficiency of a treatment, we need a reliable method to evaluate the stimulation job and to optimize future stimulation design. Related research has been carried out before by many researchers.

Glasbergen et al. (2007) and Clanton et al. (2006) developed a numerical model to obtain fluid distribution based on wellbore temperature data measured by distributed temperature sensors. Leaking of acid can be detected and this method makes real-time monitoring of stimulation possible. However, the heat transfer process they simulated is

that in the wellbore without the consideration of reaction heat and the heat transfer in the formation. Unfortunately, both of the thermal phenomenons have crucial effects on the wellbore temperature behavior.

Gao and Jalali (2005) presented an analytical solution based on a wellbore temperature model to interpret distributed temperature data in horizontal wells, from which they could create an estimated injection profile. The method is only valid for horizontal wells but not for vertical wells.

Johnson et al. (2006) noted that they interpreted distributed temperature sensors data successfully to get the flow profile for gas wells in a multilayer formation. This method relies on the Joule-Thomson effect that has great effect on gas temperature. However, this method does not work for oil wells since the Joule-Thomson effect is not significant for liquid.

Wang et al. (2008) developed a new model to determine the production profile in a multilayer formation based on the steady-state energy balance equation. This model works perfectly for both gas and oil wells. Nevertheless, this model can not solve the acid injection problem because no reaction is considered in the work.

Medeiros and Trevisan (2006) simulated the temperature profile in the formation during acid treatments. They included the reaction heat in their numerical model and successfully predict the temperature in the formation. The reservoir they considered is sandstone so that this model can not be applied for carbonate reservoir in which wormholes will be created.

1.3 Importance

We develop a numerical model to determine the temperature profile for both injection and flow back process in an acid stimulation. The method used here is similar as the one presented by previous works (Whitson and Kuntadi 2005; Glasbergen et al. 2007; Yoshioka et al. 2007; Wang et al. 2008). The governing equation is derived and solved numerically.

In this work, our model takes the heat transfer in formation and reaction heat into account, which will make the model more complete than existent ones. Besides, the wormhole growth is also considered to track the acid penetration. These results will give us a sense if the temperature could be used to diagnosis the stimulation job and to design future stimulation steps.

1.4 Objective and Procedures

The objective of this work is to develop a numerical model that is a C++ program to simulate the temperature profile for both injection and flow-back problem when acid stimulation is in process.

The procedures to conduct this research are as following:

- Derive the energy balance equations for formation fluid to be the governing equation for temperature profile.
- Couple a wormhole model with the three governing equations to track the acid penetration and include the reaction between acid and rock.

- Integrate the flow-back part into the program to achieve the temperature behavior in the wellbore.
- Study the sensitivity of flow-back temperature in the wellbore to the injection rate and other factors. Then whether the temperature is a valuable choice to diagnosis the stimulation job could be concluded.

1.5 Outline

In Section 2, the acid injection problem will be discussed. We will introduce the governing equation of the formation, Buijse's model to track the penetration, modified volumetric model to calculate the volumetric fraction of the rock that can be dissolved and how to determine the reaction term in the energy balance equation.

Section 3 will discuss the flow-back problem and what the difference is between the acid injection problem and flow-back problem.

Section 4 will show some temperature results for both injection problem and flow-back problem, based on which we can have a discussion and explanation. Some sensitivity study is also conducted in this section providing us the information that what parameters will affect the temperature behavior.

In Section 5, the results of this research will be summarized and future work will be recommended.

2. ACID INJECTION PROBLEM

2.1 Introduction

During acid injection, the heat transfer process in the formation should include heat conduction, heat convection and reaction heat. At the same time, wormholes form in the carbonate reservoirs based on fast reaction between acid and carbonate. In order to simulate the temperature behavior in the formation, both heat transfer process and wormhole penetration need to be considered.

To simplify the problem, some assumptions are made. We assume that this is a radial flow problem since it is in a vertical well. The fluid is Newtonian, incompressible fluid. Reaction only occurs at the front of wormholes which is shown as the red ring in **Fig. 2.1**. In fact, wormholes have many branches and reaction occurs along every branch instead of only at the tips. However, the main reaction is at the front of wormholes so that it is a reasonable approximation to make the problem much easier to solve.

In this section, the energy balance equation will be derived and the reaction term will be determined. Then Buijse's wormhole model will be introduced to track the wormhole growth. Modified volumetric model will be applied to calculate the dissolved rock. Finally, we show the solution and validation of this model.

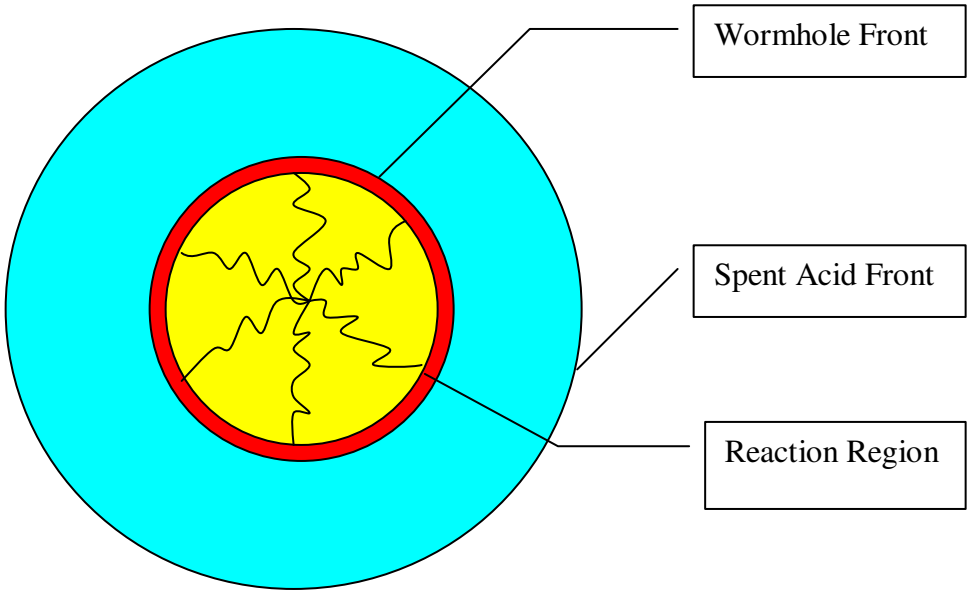

Fig. 2.1—Wormhole front and spent acid front form and reaction occurs at wormhole front

2.2 Energy Balance Equation

To simulate the temperature profile in the formation, a governing equation is required. If we apply the energy balance in a small element of formation (**Fig. 2.2**), we have the expression as

$$E_{accu} = E_{in} - E_{out} + E_{created}. \quad \text{..... (2.1)}$$

The energy that accumulates in the element can be expressed as

$$E_{accu} = \left\{\left[\rho_s \phi (e_s + e_k + e_p)\right]_{t+\Delta t} - \left[\rho_s \phi (e_s + e_k + e_p)\right]_t\right\} \times 2\pi r \Delta r \Delta z$$

$$+ \left\{\left[\rho_R (1-\phi) e_R\right]_{t+\Delta t} - \left[\rho_R (1-\phi) e_R\right]_t\right\} \times 2\pi r \Delta r \Delta z. \quad \text{..... (2.2)}$$

In the above equation, ρ_s and ρ_R are density of solution and rock respectively. ϕ is the average porosity in treated region.

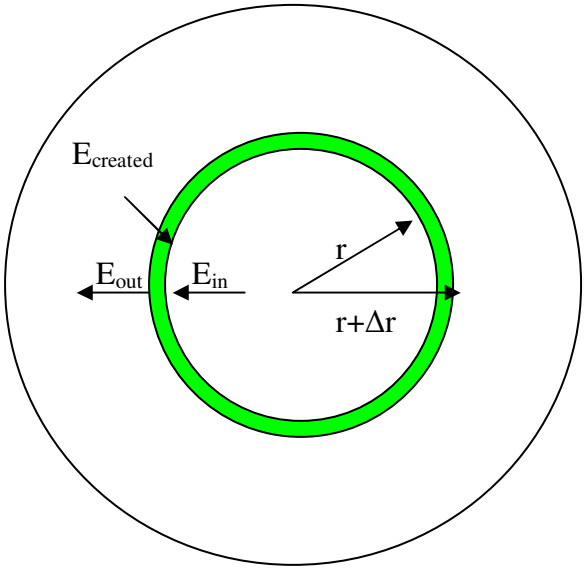

Fig. 2.2—Energy balance in the finite small element

The energy that flows into the element is

$$E_{in} = \left[\rho_s u\left(\hat{H} + e_k + e_p\right)\right]_r \times 2\pi r\Delta z\Delta t + q_r^{"} \times 2\pi r\Delta z\Delta t\,. \quad \text{..... (2.3)}$$

The energy that flows out of the element is

$$E_{out} = \left[\rho_s u\left(\hat{H} + e_k + e_p\right)\right]_{r+\Delta r} \times 2\pi(r+\Delta r)\Delta z\Delta t + q_{r+\Delta r}^{"} \times 2\pi(r+\Delta r)\Delta z\Delta t\,. \quad \text{... (2.4)}$$

The energy created by reaction is

$$E_{created} = R_i \times 2\pi r\Delta r\Delta z\Delta t \quad \text{..... (2.5)}$$

In the above equations, the specific kinetic energy, e_k, can be neglected because the difference of velocity in and out is tiny. The specific potential energy, e_P, can be neglected because this is radial horizontal flow. Then we have

$$\Delta(\rho_s\phi e_s)\times 2\pi r\Delta z\Delta r + \Delta\left[\rho_R(1-\phi)e_R\right]2\pi r\Delta r\Delta z = -\left[\Delta(\rho_s u\hat{H})\right]\times 2\pi r\Delta z\Delta t - (\rho_s u\hat{H})_{r+\Delta r}\, 2\pi\Delta r\Delta z\Delta t$$

$$-\Delta q^{"}\times 2\pi r\Delta z\Delta t - q^{"}_{r+\Delta r}\,2\pi\Delta r\Delta z\Delta t$$

$$+R_i\times 2\pi r\Delta r\Delta z\Delta t\,. \quad \text{..... (2.6)}$$

Divided Eq. 2.6 by $2\pi r\Delta r\Delta z\Delta t$, we have

$$\frac{\Delta(\rho_s\phi e_s)}{\Delta t}+\frac{\Delta[\rho_R(1-\phi)e_R]}{\Delta t}=-\frac{\Delta(\rho_s u\hat{H})}{\Delta r}-\frac{(\rho_s u\hat{H})_{r+\Delta r}}{r}-\frac{\Delta q^{"}}{\Delta r}-\frac{q^{"}_{r+\Delta r}}{r}+R_i\,. \quad \text{... (2.7)}$$

If we take the limits, $\Delta t\to 0, \Delta r\to 0$, Eq. 2.7 will become

$$\frac{\partial(\rho_s\phi e_s)}{\partial t}+\frac{\partial[\rho_R(1-\phi)e_R]}{\partial t}=-\frac{\partial(\rho_s u\hat{H})}{\partial r}-\frac{(\rho_s u\hat{H})}{r}-\frac{\partial q^{"}}{\partial r}-\frac{q^{"}}{r}+R_i\,. \quad \text{..... (2.8)}$$

Regroup Eq. 2.8, we have

$$\frac{\partial(\rho_s\phi e_s)}{\partial t}+\frac{\partial[\rho_R(1-\phi)e_R)]}{\partial t}=-\frac{1}{r}\frac{\partial(r\rho_s u\hat{H})}{\partial r}-\frac{1}{r}\frac{\partial(rq^{"})}{\partial r}+R_i\,. \quad \text{..... (2.9)}$$

$q^{"}$ is the heat flux caused by heat conduction in the formation and can be expressed as

$$q^{"}=-\lambda\frac{\partial T}{\partial r}. \quad \text{..... (2.10)}$$

$$\frac{\partial(\rho_s\phi e_s)}{\partial t}+\frac{\partial[\rho_R(1-\phi)e_R)]}{\partial t}=-\frac{1}{r}\frac{\partial(r\rho_s u\hat{H})}{\partial r}+\frac{1}{r}\frac{\partial}{\partial r}\left(r\lambda\frac{\partial T}{\partial r}\right)+R_i\,. \quad \text{..... (2.11)}$$

From the definition of enthalpy,

$$d\hat{H}=de+d(Pv)\,. \quad \text{..... (2.12)}$$

In this problem, fluid can be taken as incompressible, then

$$d\hat{H}\approx de+vdP\,. \quad \text{..... (2.13)}$$

For solid and liquid phase, specific volume v is very small, the enthalpy can be

$$d\hat{H}\approx de\approx C_p dT\,. \quad \text{..... (2.14)}$$

Finally, the energy balance equation is

$$\frac{\partial(\rho_s\phi C_{ps}T)}{\partial t}+\frac{\partial[\rho_R(1-\phi)C_{pR}T]}{\partial t}=-\frac{1}{r}\frac{\partial(r\rho_s u C_{ps}T)}{\partial r}+\frac{1}{r}\frac{\partial}{\partial r}\left(r\lambda\frac{\partial T}{\partial r}\right)+R_i. \quad \text{..... (2.15)}$$

In Eq. 2.15, ρ is density, C_p is the heat capacity, T is temperature, u is the velocity of fluid in the formation, and λ is the heat conductivity for both acid solution and rock.

In the left hand side of Eq. 2.15, we have accumulation term for both rock and acid solution. In the right hand side, the first time is heat convection term which is also the dominating term in this problem. The second term is heat conduction term which considers the heat conducted in solution and rock. The last term is reaction term and can not be expressed analytically.

2.3 Reaction between Acid and Rock

During acidizing treatments in carbonate reservoirs, the injected acid enters formation and wormhole forms accompanied with reaction. Wormholes have branching-like structures and reaction occurs along each branch, which is difficult to simulate. In this work, we make assumption that the reaction only occurs at the front of wormholes.

To determine the reaction term in the energy balance equation, we need to decide two factors. The first one is the amount of acid consumed in the reaction, which also means the amount of rock that is dissolved. This factor will be discussed in the following section. The second one is the reaction heat released when unit mole of acid is consumed.

Assuming the reservoir rock is calcite ($CaCO_3$) and acid used is hydrochloric acid, the reaction formula is

$$CaCO_3 + 2HCl \rightarrow CaCl_2 + H_2O + CO_2 . \quad \text{..... (2.16)}$$

The reaction heat for unit mole hydrochloric acid can be calculated by

$$Q_{reac} = \sum \left|\Delta H(\text{reactants})\right| - \sum \left|\Delta H(\text{resultants})\right| . \quad \text{..... (2.17)}$$

The enthalpies of reactants and resultants are listed in **Table. 2.1**.

Table 2.1 Enthalpy of Reactants and Resultants (Perry et al. 1963)

Substance	ΔH, kcal/mol
$CaCO_3$	-289.5
HCl	-39.85
$CaCl_2$	-209.15
H_2O	-68.32
CO_2	-94.05

The reaction heat for unit mole acid is

$$Q_{reac} = 2.32 kcal/(molCaCO_3) = 1.16 kcal/(molHCl) . \quad \text{..... (2.18)}$$

Applying SI unit system, we have

$$Q_{reac} = 9.71 kJ/(molCaCO_3) = 4.855 kJ/(molHCl) . \quad \text{..... (2.19)}$$

2.4 Wormhole Growth Model

In this work, Buijse's wormhole model will be used to track the wormhole growth. Buijse's model is a semiempirical model and is considered more accurate than

others. Modified volumetric model will be applied to calculate the amount of rock that is dissolved by acid, which will be introduced in the next subsection.

In Buijse's wormhole model, the velocity of wormhole growth in radius geometry can be expressed as

$$V_{wh}(R_{wh}) = W_{eff} \cdot V_i(R_{wh})^{2/3} \cdot B(V_i(R_{wh})) \cdot D(t). \quad \text{..... (2.20)}$$

In Eq.2.20, $V_i(R_{wh})$ is the interstitial acid velocity in formation, and defined by

$$V_i(R_{wh}) = \frac{Q}{2\pi R_{wh} h \cdot \phi}. \quad \text{..... (2.21)}$$

Q is the total volume injected and R_{wh} is the wormhole radius. h is the thickness of the formation and ϕ is the porosity.

$B(V_i)$ is the B-function and the expression for it is

$$B(V_i) = \left(1 - \exp(-W_B \cdot V_i^2)\right)^2. \quad \text{..... (2.22)}$$

$D(t)$ is a step function,

$$D(t) = 1 - \exp\left(-\left(\frac{t}{W_t}\right)^{10}\right). \quad \text{..... (2.23)}$$

W_{eff}, W_B and W_t are constants that can be determined by experiments. Approximately, W_t is equal to 1. W_{eff} and W_B can be calculated by Eqs. 2.24 and 2.25,

$$W_{eff} = \frac{V_{i-opt}^{1/3}}{PV_{bt-opt}}. \quad \text{..... (2.24)}$$

$$W_B = \frac{4}{V_{i-opt}^2}. \quad \text{..... (2.25)}$$

V_{i-opt} is the optimum interstitial velocity and PV_{bt-opt} is the optimum breakthrough pore volumes. Both of the parameters are treated as the input variables in the model. Generally the optimum interstitial velocity and optimum breakthrough pore volumes should be determine by core tests. A typical relation between them for some combinations of acid and rock is shown in **Fig. 2.3**. From the minimum point of the curve, we can obtain the optimum values as our input data.

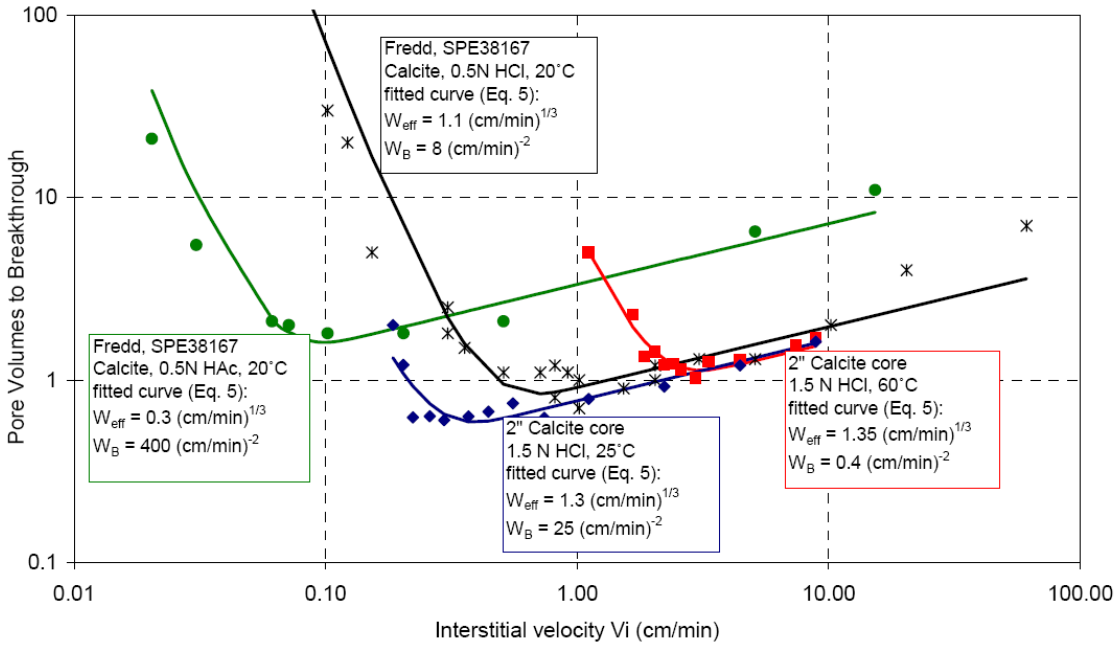

Fig. 2.3— Core flow test results. Pore volumes to breakthrough as a function of injection rate. (Buijse and Glasbergen 2005)

Then a suitable scheme to perform this calculation can be developed:

1. divide the total pump time in small time step Δt
2. start with $R_{wh}(t=0) = r_w$ (wellbore radius) and loop through the flowing steps
3. calculate V_i from R_{wh} (t), using Eq. 2.21

4. calculate V_{wh} from Eq. 2.20
5. use V_{wh} to calculate a new value for R_{wh} at time t+Δt by Eq. 2.26

$$R_{wh}(t+\Delta t) = V_{wh} \cdot \Delta t + R_{wh}(t). \quad \text{..... (2.26)}$$

6. back to step 3 and repeat same calculates for $R_{wh}(t+\Delta t)$

2.5 Modified Volumetric Model

From Buijse's model, the pore volumes to breakthrough the core sample can be calculated by

$$PV_{bt}(t) = \frac{V_i(t)^{1/3}}{W_{eff} \cdot B(V_i(t))}. \quad \text{..... (2.27)}$$

Economides et al. (1994) presented the wormhole efficiency which can be calculated by

$$\eta(t) = N_{AC}(t) PV_{bt}(t). \quad \text{..... (2.28)}$$

In the original model, wormhole efficiency and break through pore volumes are considered as constants. However, it is not what happens in the wormholes. Here we define them as functions of time.

N_{AC} is the acid capacity number that can be expressed as

$$N_{AC}(t) = \frac{\phi(t)\beta_F C_{HCl}^0 \rho_s}{(1-\phi(t))V_F^0 \rho_R}. \quad \text{..... (2.29)}$$

β_F is the dissolving power of the acid, C_{HCl}^0 is acid concentration in weight fraction and V_F^0 is the volumetric fraction of fast-reaction rock.

The volume of rock has been dissolved is

$$V_{dis}(t) = \eta(t) \cdot \pi \left[R_{wh}(t + \Delta t)^2 - R_{wh}(t)^2 \right] \cdot h(1 - \phi_i) . \quad \text{..... (2.30)}$$

The mole of HCl that consumed by reaction is

$$n_{HClcon}(t) = \frac{2 \cdot V_{dis}(t) \cdot \rho_R}{M_R} . \quad \text{..... (2.31)}$$

M_R is the molecular mass of rock.

Then we can figure out reaction terms for governing equations numerically,

$$R_i(t) = \frac{n_{HClcon}(t) \times Q_{reac}}{2\pi r \Delta r \Delta z \Delta t} . \quad \text{..... (2.32)}$$

2.6 Solution of Acid Injection Problem

Since there is no analytical expression for reaction term, the energy balance equation can not be solved analytically. The only choice is to solve it numerically. The discretized energy balance equation is

$$\frac{\left(\rho_s \phi C_{ps} T\right)_m^{p+1} - \left(\rho_s \phi C_{ps} T\right)_m^p}{\Delta t} + \frac{\left[\rho_R (1-\phi) C_{pR} T\right]_m^{p+1} - \left[\rho_R (1-\phi) C_{pR} T\right]_m^p}{\Delta t}$$

$$= -\frac{1}{r_m} \cdot r_w u_w \cdot \frac{\left(\rho_s C_{ps} T\right)_{m+1}^{p+1} - \left(\rho_s C_{ps} T\right)_{m-1}^{p+1}}{2\Delta r} + \frac{\lambda}{r_m} \frac{(T)_{m+1}^{p+1} - (T)_{m-1}^{p+1}}{2\Delta r}$$

$$+ \lambda \frac{T_{m+1}^{p+1} - 2T_m^{p+1} + T_{m-1}^{p+1}}{\Delta r^2} + R_i . \quad \text{..... (2.33)}$$

r_w is the wellbore radius. u_w is the velocity of acid solution at wellbore, which could be calculated directly from the injection rate. The reaction term R_i is calculated as mentioned in the last subsection.

To solve the discretized equation, some assumptions need to be made. We assume this is a 1D radial flow problem for single layer and the injection rate keeps a constant. Besides, the thermal radiation, Joule-Thompson effect and heat caused by friction are neglected here since they do not have significant effect on the temperature behavior. For fluid, we assume it is Newtonian, incompressible fluid.
Furthermore, we have the boundary and initial conditions as following,

$$\begin{aligned} &T(\infty,t) = T_g \\ &T(r_w,t) = T_a \ , \\ &T(r,0) = T_g \end{aligned} \quad \text{..... (2.34)}$$

where T_g is the geothermal temperature at the layer's depth and T_a is the temperature of injected acid.

A program is developed to solve the energy balance equation numerically and the flow chart is shown below **(Fig. 2.4)**.

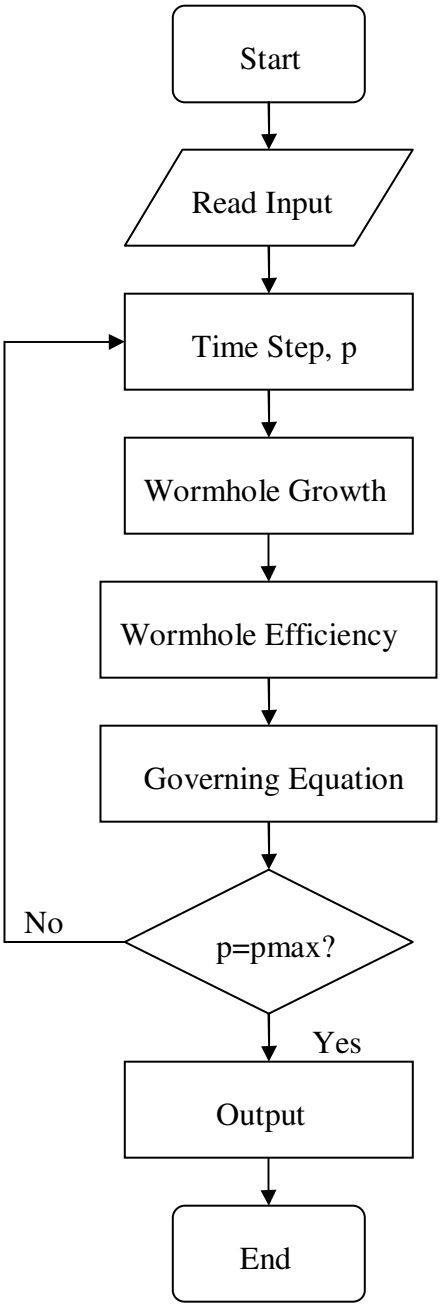

Fig. 2.4—Flow chart for programming acid injection problem

2.7 Validation of Injection Model

To ensure the injection model works, we prefer to achieve a match between our model and some published results. Medeiros and Trevisan (2006) presented their simulation results for the acid injection problem in sandstone reservoir (**Fig. 2.5**). They do not have wormhole models and they assume 20% of the calcite will be dissolved by HCl. Using the same conditions, we simulated the temperature behavior during an acid injection process, and result is shown is **Fig. 2.6**.

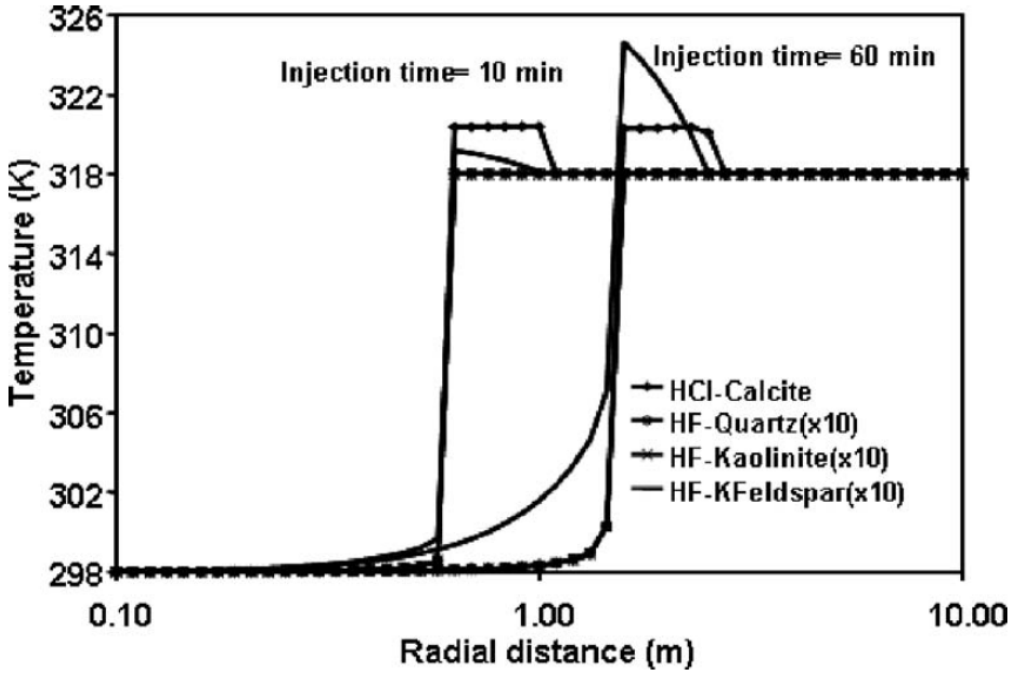

Fig. 2.5—Temperature in the formation for a constant injection temperature of 298 K (Medeiros and Trevisan 2006)

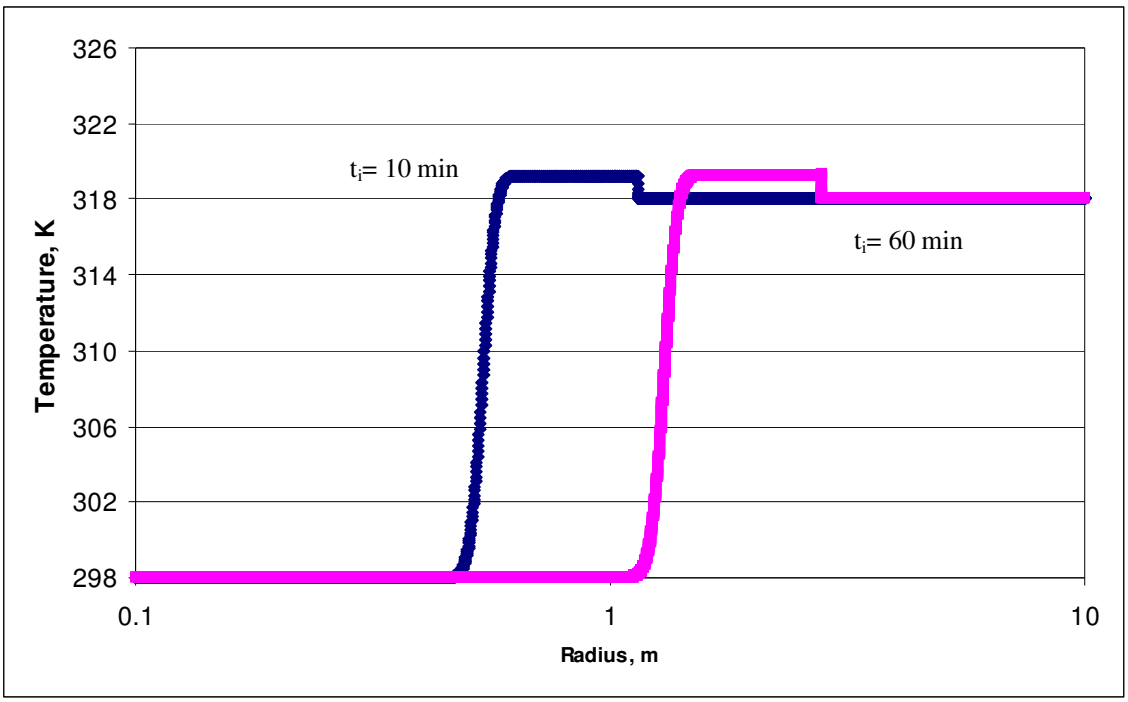

Fig. 2.6—Temperature simulated by our model for the same case

Comparing **Fig. 2.5** and **Fig. 2.6**, we achieved a good match between our simulation result and the result they presented although the temperature peak is not exactly the same, which is because the approaches to calculate reaction heat are very different.

This match proves that our acid injection model is valid, which is the base of flow-back problem.

2.8 Section Summary

In this section, we discuss the acid injection problem. The energy balance equation, reaction between acid and rock and wormhole model are introduced. The

solution of injection problem matched the result from some published papers, and validating my acid injection model. The acid injection problem is the base for flow back problem, which will be discussed in the next section.

3. FLOW-BACK PROBLEM

3.1 Introduction

The temperature that can be measured usually is the temperature in the wellbore rather than the temperature profile in the formation since the distributed temperature sensors are most likely installed at the wellbore, between tubing and casing. To use the temperature data to interpret a flow profile, we need a flow back model to examine if the temperature peak still exits.

In the flow-back problem, the initial condition is the temperature profile we achieved from the acid injection problem. We also assume constant flow-back rate. For energy balance equation, we neglect the heat conduction since this heat transfer process is dominated by heat convection. Reaction heat does not exist in the flow-back problem because we assume that the acid has been spent and lose the dissolving power during the injection.

3.2 Governing Equation

The governing equation is the energy balance equation as well. The velocity is also calculated directly from the constant flow-back rate.

In the same process as injection problem, we can conduct energy balance to an element in the reservoir and remember there is no heat conduction and reaction heat. Then the energy balance equation for flow-back problem is

$$\frac{\partial(\rho_s \phi C_{ps} T)}{\partial t} + \frac{\partial[\rho_R (1-\phi) C_{pR} T]}{\partial t} = -\frac{1}{r}\frac{\partial(r \rho_s u C_{ps} T)}{\partial r}. \quad \text{..... (3.1)}$$

3.3 Solution of Flow-Back Problem

The flow-back problem, there are two possible ways to solve the equation, either analytically or numerically.

For both of the solving method, the boundary and initial conditions are shown as Eq. 3.2

$$\begin{aligned} T(\infty, t) &= T_g \\ T(r, 0) &= T_i(r) \end{aligned}. \quad \text{..... (3.2)}$$

$T_i(r)$ is the temperature distribution as a function of radius at the last time step we got from acid injection problem. Since we neglect the heat conduction term, we only need one boundary condition. The temperature in the wellbore is what we want to simulate because distributed temperature sensors can only measure the temperature at the wellbore.

To get the analytical solution, we assume that density of rock and acid solution, the porosity, and heat capacity are all constants. Then Eq.3.1 becomes

$$\left[1 + \frac{\rho_R C_{pR} (1-\phi)}{\rho_s C_{ps} \phi}\right] \frac{\partial T}{\partial t} = -\frac{r_w u_w}{\phi} \frac{1}{r} \frac{\partial T}{\partial r}. \quad \text{..... (3.3)}$$

If we define

$$A = 1 + \frac{\rho_R C_{pR} (1-\phi)}{\rho_s C_{ps} \phi}, \quad \text{..... (3.4)}$$

$$B = -\frac{r_w u_w}{\phi}, \quad \text{..... (3.5)}$$

The equation becomes

$$A\frac{\partial T}{\partial t} = B\frac{1}{r}\frac{\partial T}{\partial r}. \quad \text{..... (3.6)}$$

The solution of the above PDE is

$$T(r,t) = T_i\left(\sqrt{r^2 + \frac{2B}{A}t}\right). \quad \text{..... (3.7)}$$

However, the reaction term in the energy balance equation can not be expressed explicitly thus there is no analytical solution for the acid injection problem, which means the analytical solution for the low-back problem is not valuable here.

To get the numerical solution, we still discretize the governing equation first. The discretized equation for Eq. 3.1 is

$$\frac{\left(\rho_s \phi C_{ps} T\right)_m^{p+1} - \left(\rho_s \phi C_{ps} T\right)_m^{p}}{\Delta t} + \frac{\left[\rho_R (1-\phi) C_{pR} T\right]_m^{p+1} - \left[\rho_R (1-\phi) C_{pR} T\right]_m^{p}}{\Delta t}$$

$$= -\frac{1}{r_m} \cdot r_w u_{well} \cdot \frac{\left(\rho_s C_{ps} T\right)_{m+1}^{p+1} - \left(\rho_s C_{ps} T\right)_{m-1}^{p+1}}{2\Delta r}. \quad \text{..... (2.32)}$$

The flow chart for the program of numerically solution is shown as **Fig. 3.1**.

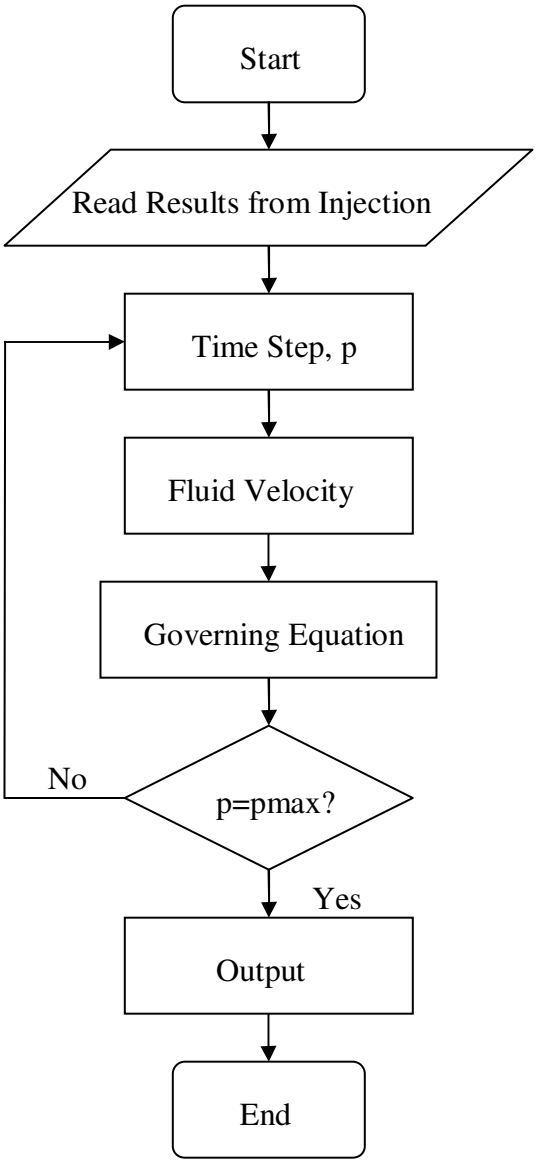

Fig. 3.1—Flow chart for programming flow-back problem

3.4 Section Summary

In this section we discussed the flow-back problem and derive the energy balance equation. The only difference between flow-back problem and injection problem is that we do not have reaction in the formation and also we neglect the heat conduction since it is insignificant. We investigated the possibility of the analytical solution, but it is not applied since it depends on the analytical solution of the injection problem which we can not obtain. Finally, the numerical method is presented.

4. RESULTS AND DISCUSSION

4.1 Introduction

After simulation, we can find the numerical solution of the model. In this section, we will discuss the results of acid injection problem and flow-back problem to determine if temperature can provide us enough information to identify the acid flow profile.

The results are first shown for two cases; injection rate is 0.5 bbl/min and 1 bbl/min. After that, some sensitivity study is conducted to discuss the factors that affect the temperature behavior.

4.2 Temperature Profile during Injection

A synthetic case is used to show the temperature simulation results from the model. All the input data are for example listed in **Table. 4.1**.

After the simulation, we can achieve the temperature distribution in the formation. The results shown here are for two different injection rates and two different injection times.

Figure 4.1 presents the temperature profile for the injection problem. There are three sections in temperature profile. The first section is 298 K, which is the temperature of injected acid. The second is the temperature peak caused by reaction heat released by acid reacting with carbonate. The last section starts when the peak drops to the reservoir temperature, which is also geothermal temperature at the depth of this layer.

Table 4.1 Input Data	
Parameters	Value
C_{HCl}(weight fraction)	15%
C_{pR}, J/(kg·K)	1040
C_{ps}, J/(kg·K)	4186.8
h, ft	10
M_R, kg/mol	0.1
q, bbl/min	0.5
	1
Q_{reac}, J/(molHCl)	4855
r_w, ft	0.583
t_i, min	10
	20
t_f, min	20
T_e, K	318
T_i, K	318
T_a, K	298
ρ_R, kg/m^3	2150
ρ_s, kg/m^3	1080
λ, W/(m·k)	3.6
V_{iopt}, m/s	0.00015
PV_{btopt}	0.95
Φ_i	0.2
β_F	1.37

Figure 4.2 shows the temperature with two injection rates. It demonstrates that for greater injection rate, the acid will penetrate deeper. Besides, the peak of temperature in the formation is higher. When more acid enters the layer, more carbonate will be dissolved and more reaction heat will be released during the acid injection process.

In **Fig. 4.3**, temperature behaviors for two different injection times are displayed. The injection rate is 0.5 bbl/min. For longer injection time, the peak will drop and become “fatter”. The reason for this is the heat conduction. The heat conduction in the formation will transfer the reaction heat in both of the directions and disperse the temperature peak.

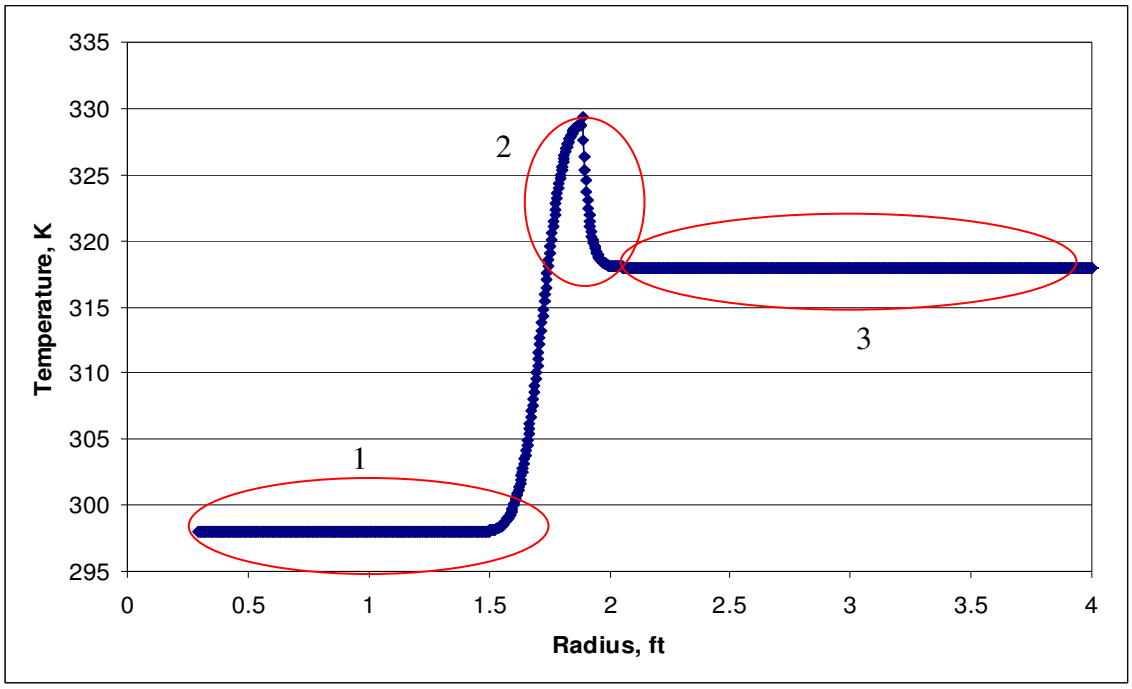

Fig. 4.1—Temperature distribution in the formation for q=1 bbl/min after injecting for 10 min

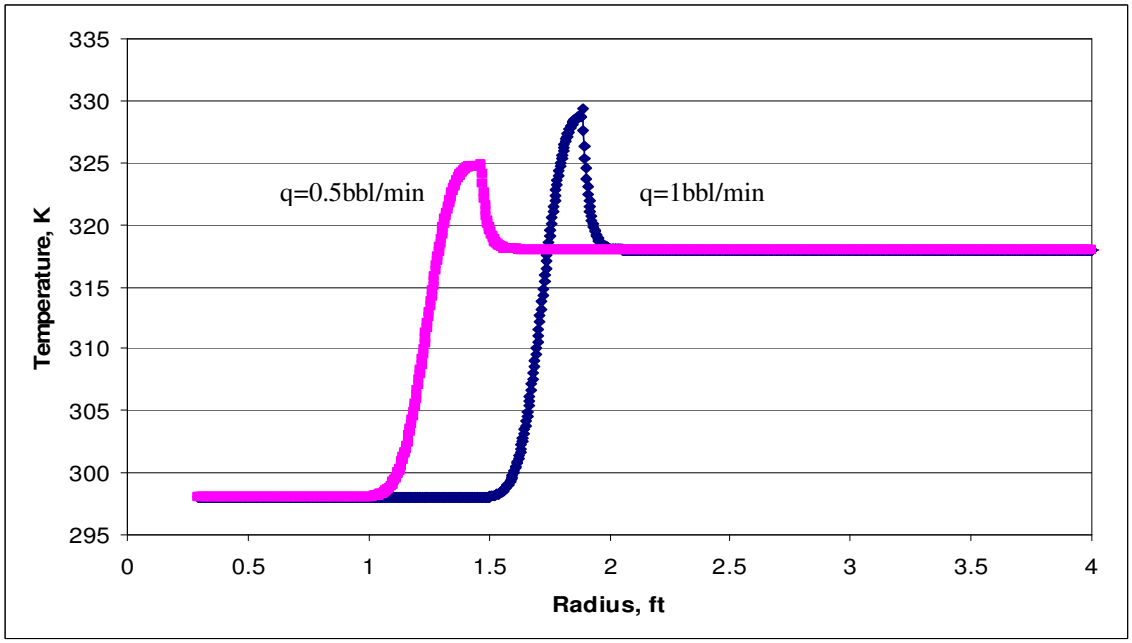

Fig. 4.2—Temperature distribution in the formation for different injection rate after injecting for 10 min

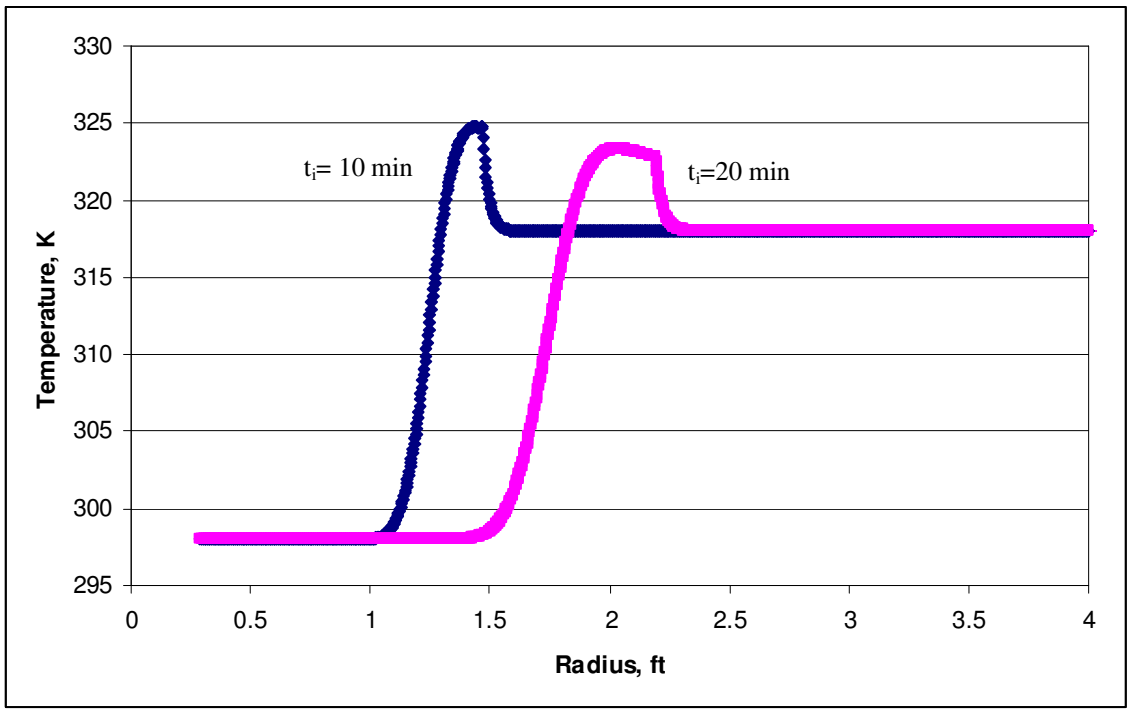

Fig. 4.3—Temperature distribution in the formation for different injection time when q=0.5 bbl/min

Comparing **Fig. 4.3** and **Fig. 4.4**, different injection rates give us different velocities of acid, which affect the heat convection. Then the shape of the temperature peak varies.

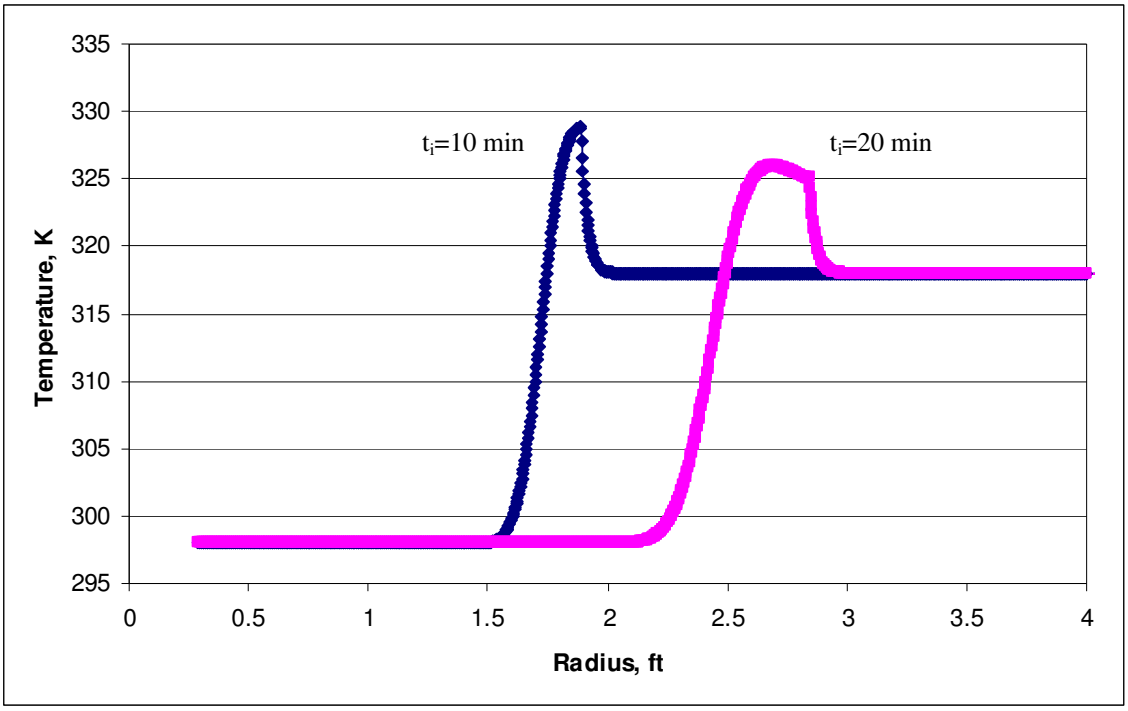

Fig. 4.4—Temperature distribution in the formation for different injection time when q=1 bbl/min

Wormhole front and spent acid front are presented in **Fig. 4.5**. The spent acid front is ahead of the wormhole front in this case based on the optimum interstitial velocity and the optimum breakthrough pore volumes we input to the model. The breakthrough pore volumes calculated for each time step is greater than 1 as the reason for that the spent acid front is ahead of the wormhole front. The break through pore volumes is considered as a function of time, showing in **Fig. 4.6**. It decreases with time since it is proportional to $V_i^{1/3}$. The wormhole efficiency, the volumetric fraction of dissolved rock, also decreases with time **(Fig. 4.7)** for the reason that the acid is consumed along the wormhole as it forms. When acid goes further and further, the concentration of HCl decreases and wormhole efficiency decreases as well.

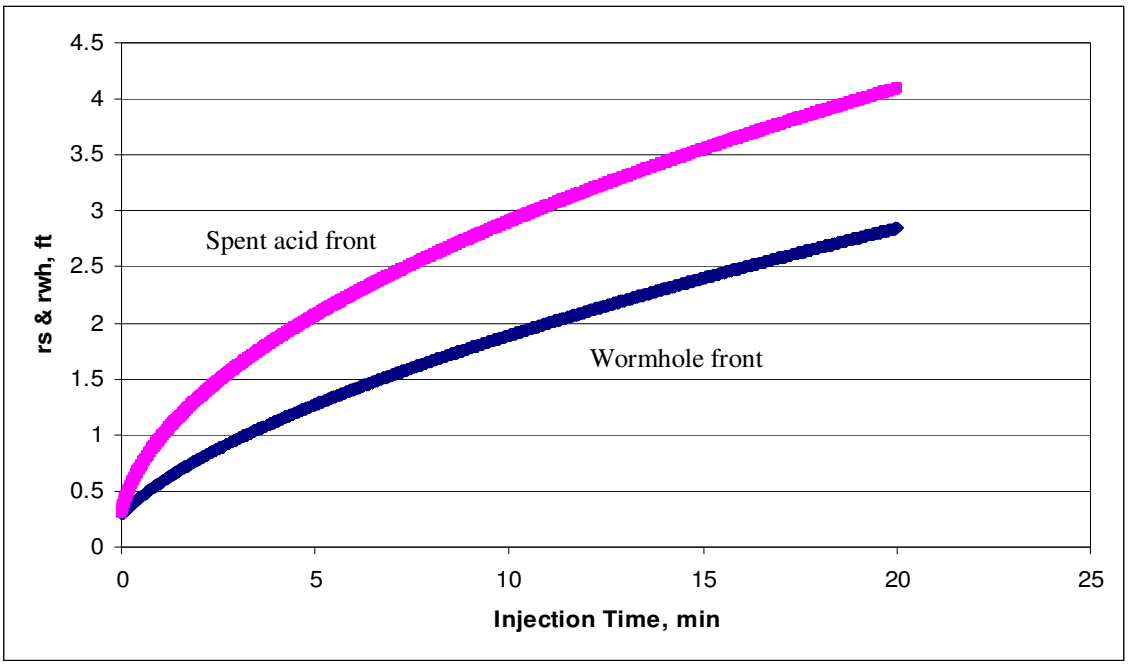

Fig. 4.5—Wormhole front and spent acid front when q= 1 bbl/min

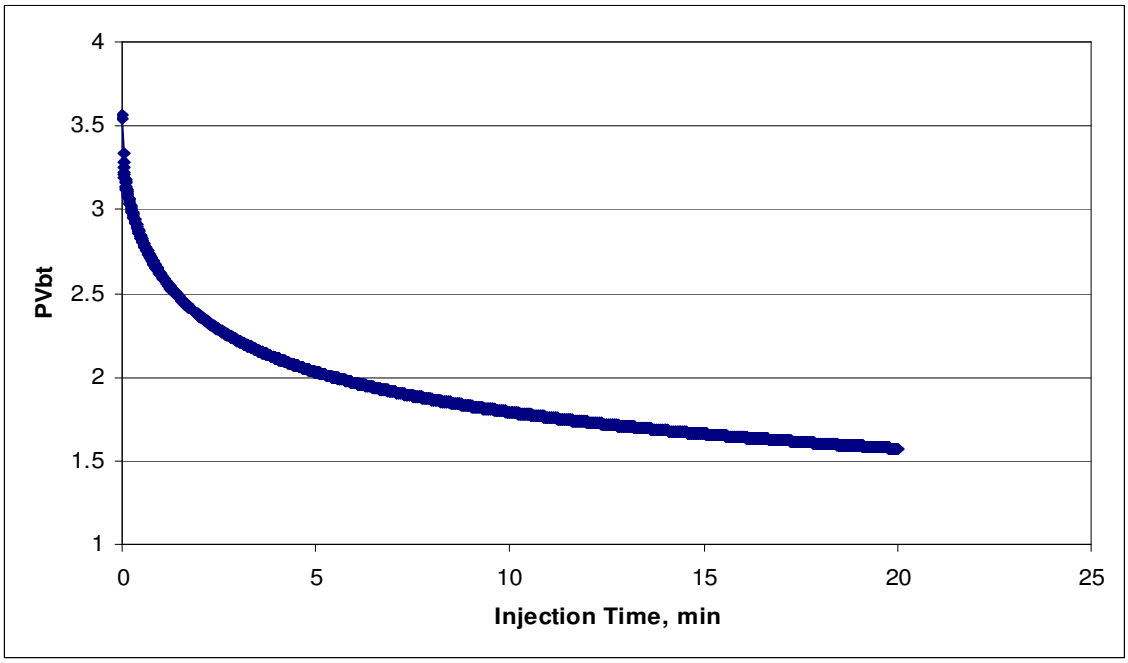

Fig. 4.6—Break through pore volumes as a function of time greater than 1 when q=1 bbl/min

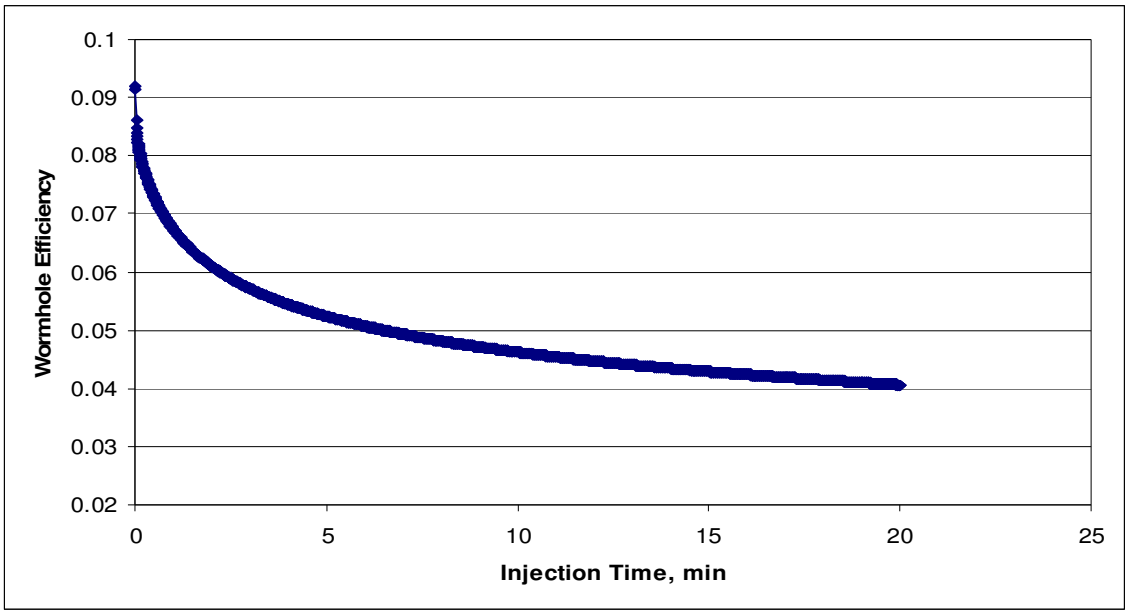

Fig. 4.7—Wormhole efficiency as a function of time when q=1 bbl/min

The average porosity of treated formation will increased first since the more pore volume is created by reaction, which is shown as the first part of the curve in **Fig. 4.8**. After that, since the wormhole efficiency decreases all the time, then the pore volume created every time step by reaction decreases as well. Besides, the treated region is increasing. However, the average porosity is still greater than the original porosity.

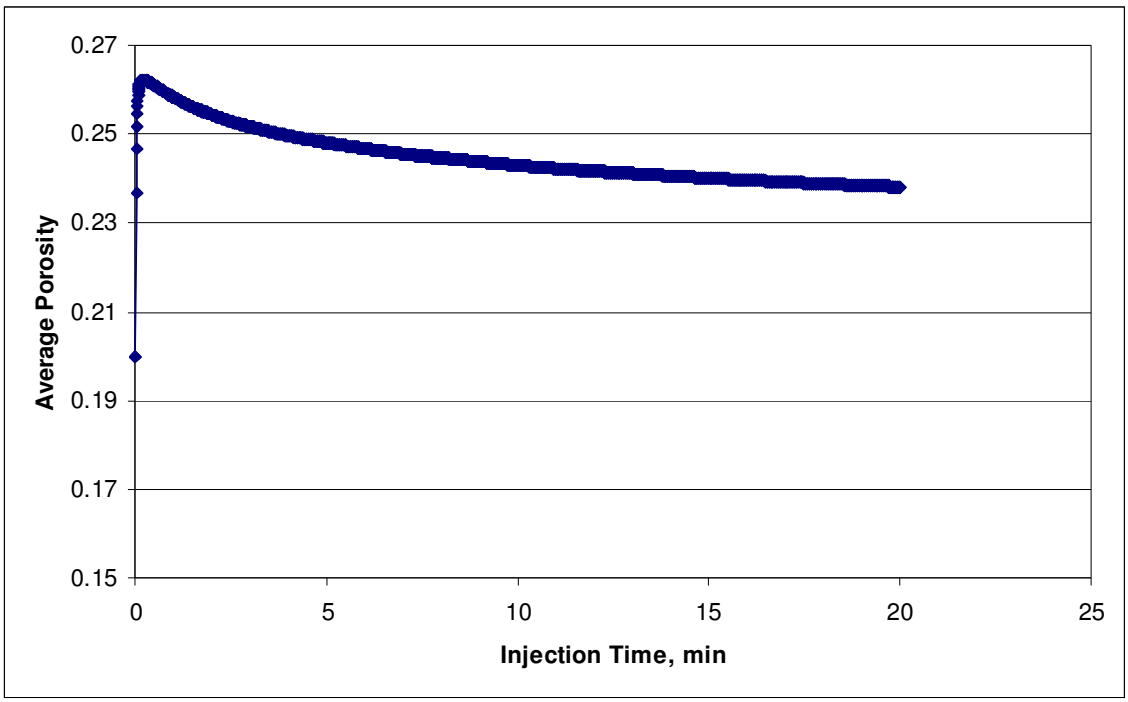

Fig. 4.8—Average porosity of treated formation as a function of time when q=1 bbl/min

4.3 Temperature Profile during Flowing Back

Using the temperature profile obtained in the acid injection problem as the initial condition, we can simulate the temperature profile in the formation when the well is flowing back.

Figure 4.9 shows that when the well is flowing back, the acid injected will enter the well first, followed by the formation fluid with the geothermal temperature at this depth. The temperature peak caused by reaction should arrive at the wellbore between them in time.

If the injection rate and flow-back flow rate is higher, the temperature peak will arrive at the wellbore faster, which is clearly shown comparing **Fig. 4.9** and **Fig. 4.10**.

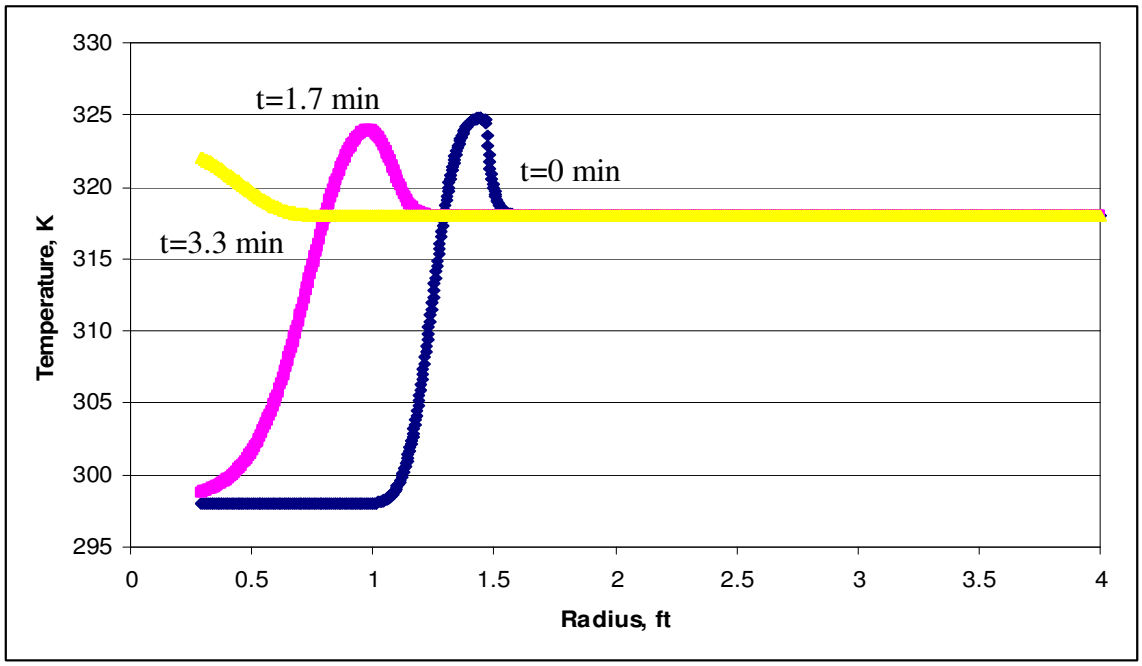

Fig. 4.9—Temperature profile in the formation when the well is flowing back at 0.5 bbl/min after injection for 10 min (0.5bbl/min)

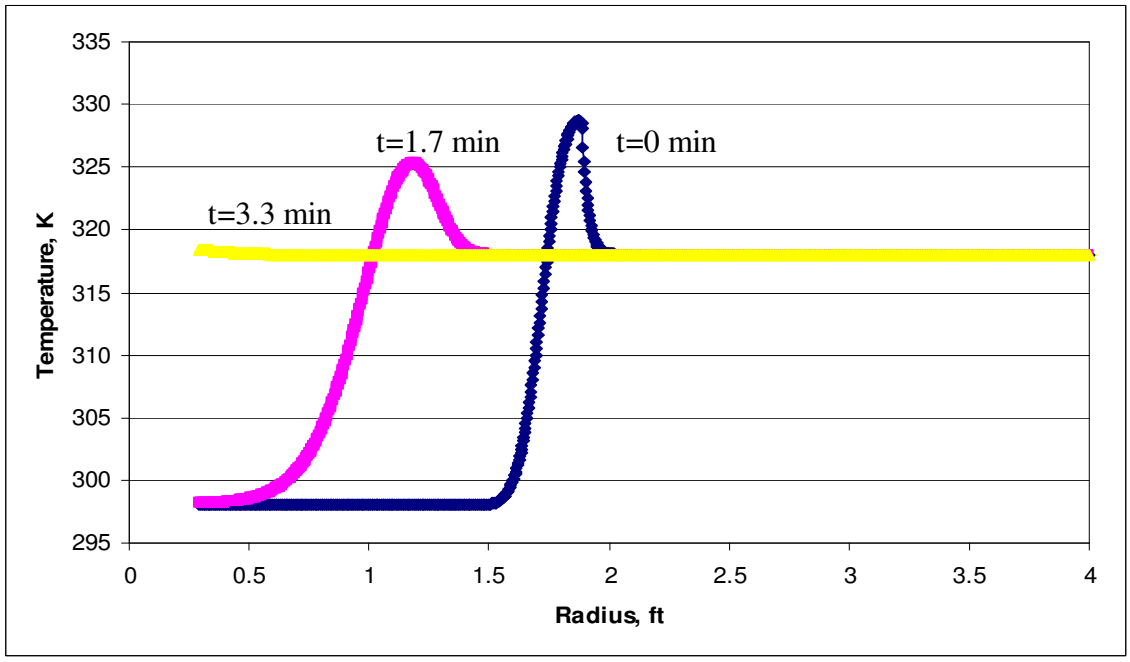

Fig. 4.10—Temperature profile in the formation when the well is flowing back at 1 bbl/min after injection for 10 min (1 bbl/min)

Figure 4.11 presents the temperature profile after injection for 20 min. With longer injection time, the acid will penetrate deeper, and therefore it takes longer time to flow the acid and temperature peak back to the wellbore. Besides, the temperature peak is becoming wider because if the total reaction heat is constant, the radius range for temperature peak is larger since this is a radial flow problem.

Figure 4.12 is plotting the wellbore temperature as a function of time. For different injection rate, we have different wellbore temperature behavior, not only the value of the peak, but also the time when the peak reaches the wellbore. All these differences are caused by reaction, which gives us a mechanism to quantitatively determine the acid flow profile.

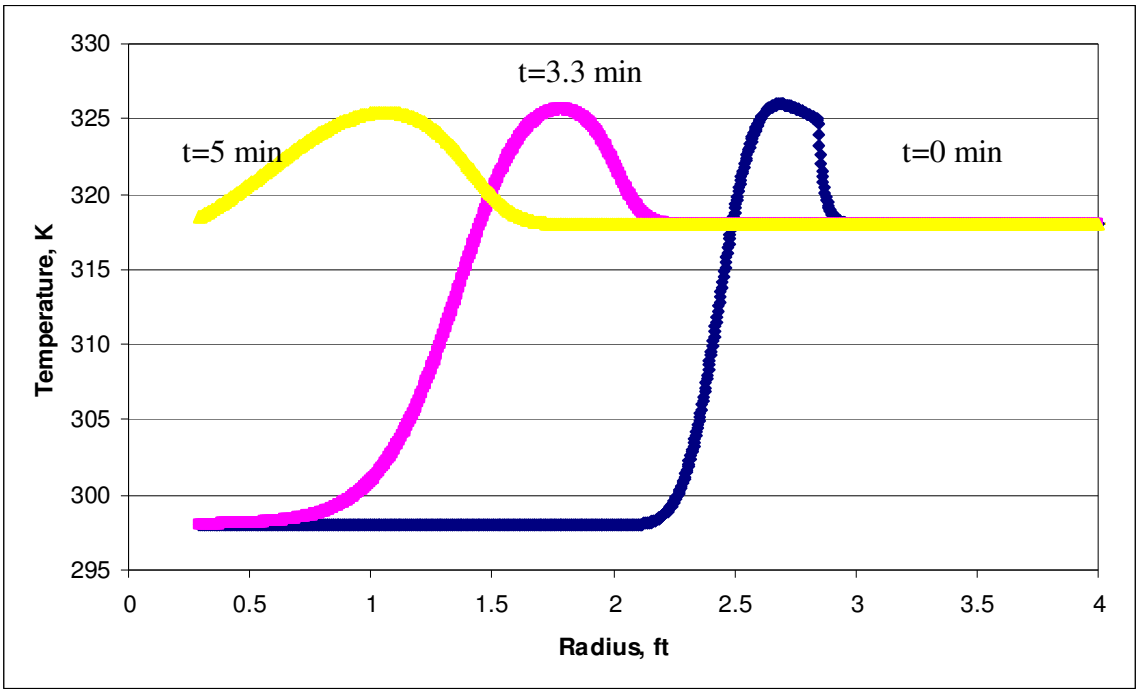

Fig. 4.11—Temperature profile in the formation when the well is flowing back at 1 bbl/min after injection for 20 min (1 bbl/min)

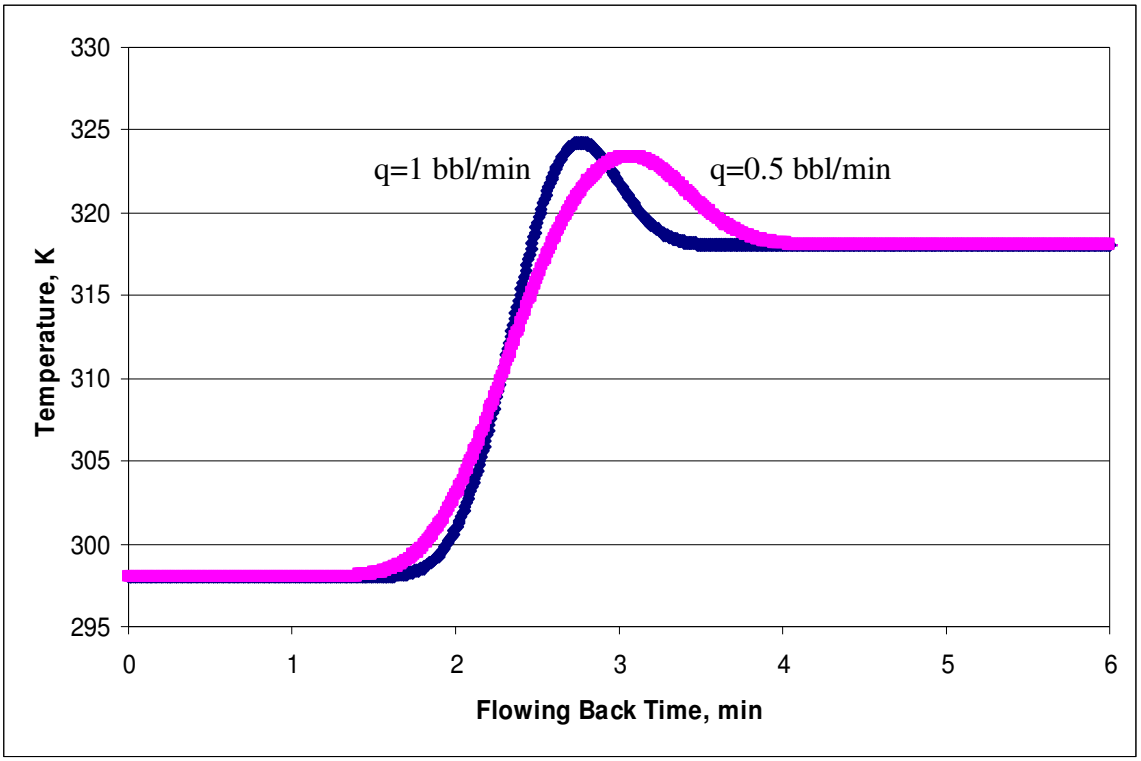

Fig. 4.12—Temperature measured at the wellbore for different flow rate after 10 min injection

4.4 Sensitivity Study

Besides the injection rate, there are other parameters affecting the temperature behavior. Sensitivity study on initial porosity and heat conductivity will be conducted in the subsection.

Varying initial porosity from 0.15 to 0.25, all the temperature behaviors for injection problem are shown in **Fig. 4. 13**. For smaller porosity, acid penetrates with a higher velocity and with the same injection time, acid penetrates deeper. Besides, the

reaction region we assumed is larger which is going to be heated by reaction heat. That is the reason we have lower peak for ϕ_i=0.15.

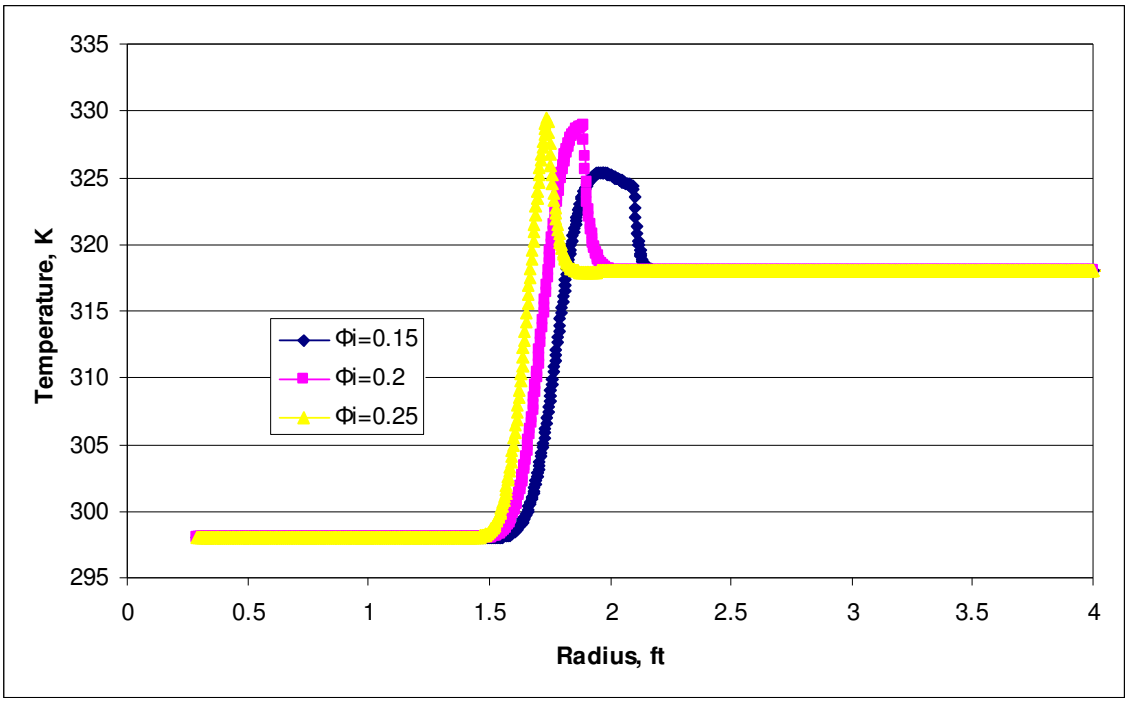

Fig. 4.13—Comparison of injection temperature profile for different porosity

For the flow-back problem (**Fig. 4.14**), since the flow-back velocity is also larger for smaller porosity, the distance between three peaks decreases. Another thing need to be noticed is that the temperature peak for the largest porosity is the lowest although during injection it has the highest peak. This is caused by the reaction heat. For ϕ_i=0.25, the amount of rock that can be dissolved is small so that the reaction heat released is small as well. During injection, this reaction heat only needs to heat up a small reaction

region and shows larger temperature increase. During flowing back, the peak will be reduced because the small amount of reaction heat.

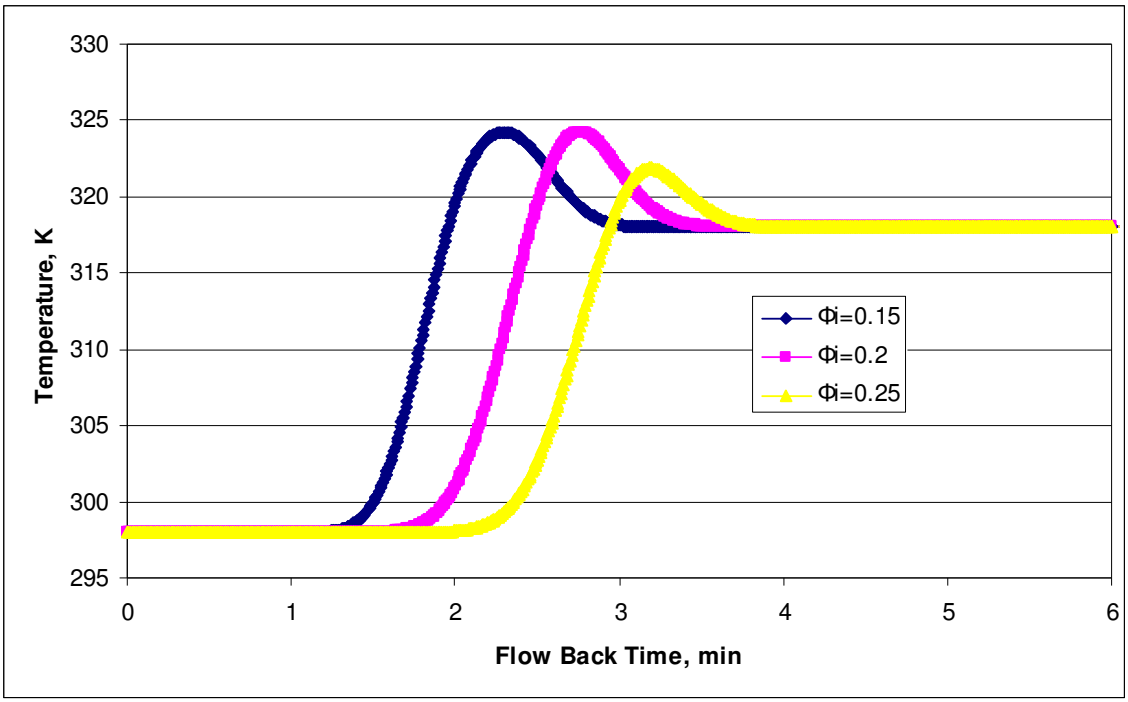

Fig. 4.14—Comparison of wellbore temperature profile for different porosity

From **Fig. 4.15** and **Fig. 4.16**, we can see that heat conductivity for both rock and solution does not have great effect on the temperature behavior. Only the height of the peak changes a little because more heat is dispersed by heat conduction. This also proves that heat convection is dominating in this heat transfer process.

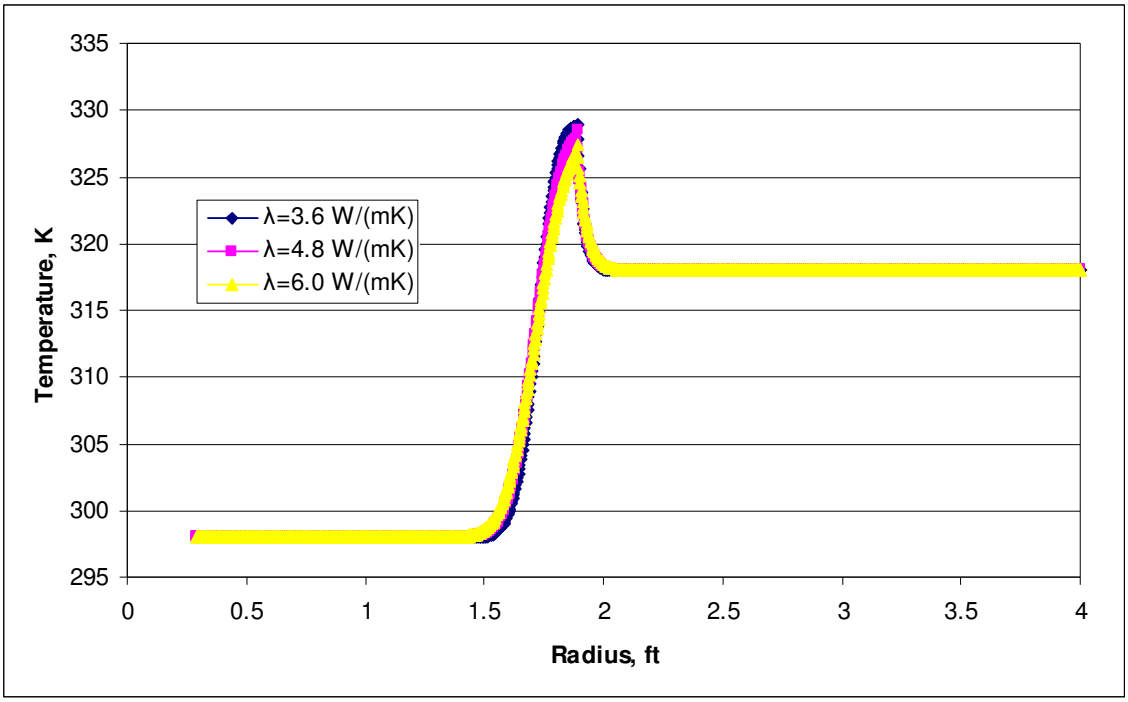

Fig. 4.15—Comparison of injection temperature profile for different heat conductivity

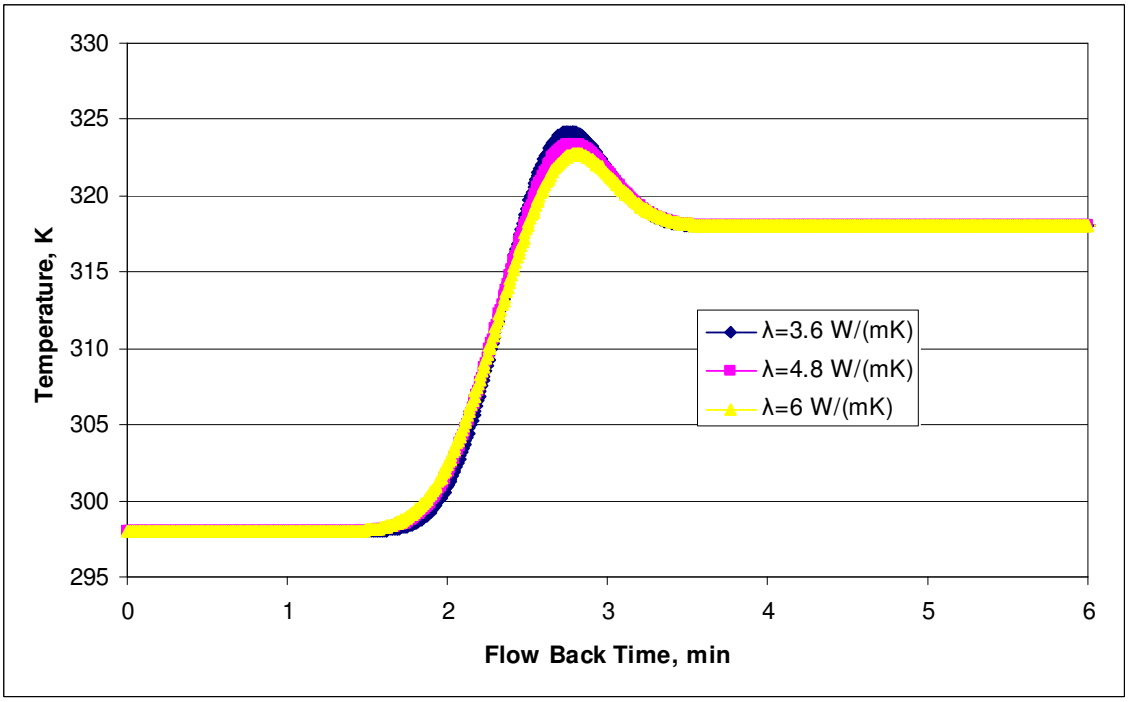

Fig. 4.16—Comparison of wellbore temperature profile for different heat conductivity

Figure 4.17 shows the sensitivity of wellbore temperature to the injection rate. The flow-back rate is assumed the same as injection rate. We observe that for just a little change of the injection rate, we have obvious deviation of the temperature behavior. This gives us more confidence for the future work.

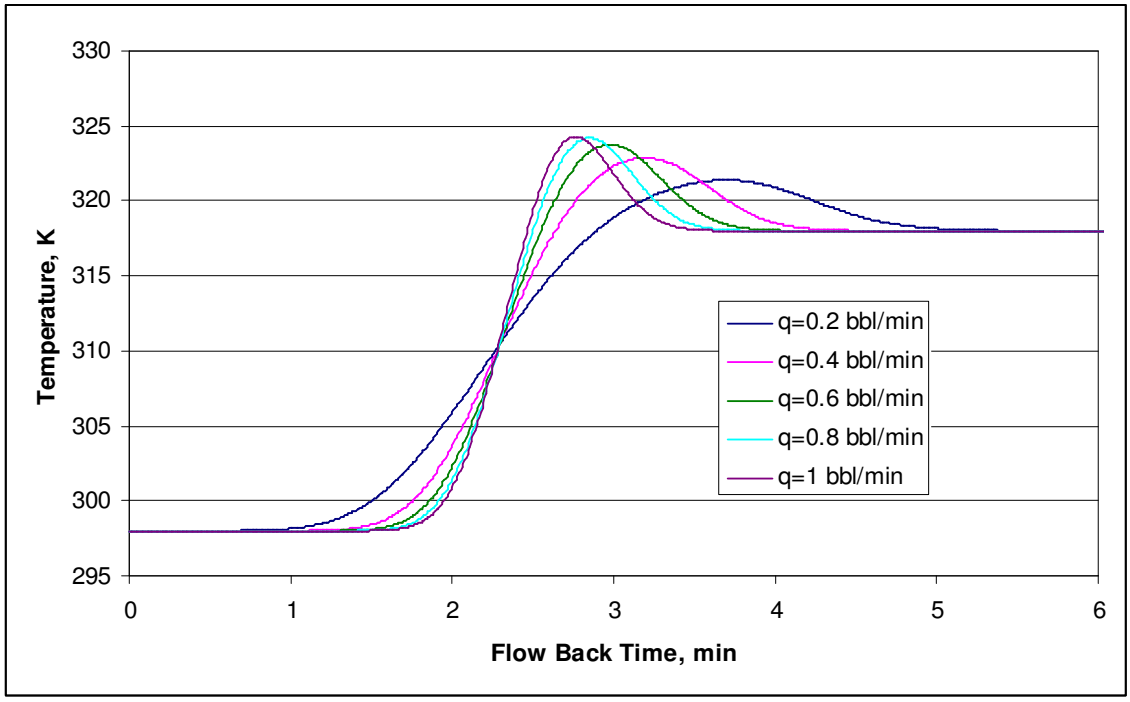

Fig. 4.17—Comparison of wellbore temperature profile for different injection rate

4.5 Section Summary

In this section, we showed the results for injection problem and flow-back problem. For injection problem, we have three parts of the curve: acid temperature, reaction peak and geothermal temperature. For flow-back problem, we still have these three parts and peak disperses with time. The most significant thing is we have different

temperature behaviors for different injection rates and this provide us a method to quantify the acid flow profile.

5. CONCLUSIONS AND RECOMMENDATIONS

5.1 Conclusions

Combining the energy balance equation, Buijse's wormhole model and modified volumetric wormhole model, we developed a new model to simulate the heat transfer process in the formation during acid injection and flowing back. Heat conduction, heat convection and reaction heat are all considered. With this model, it was found:

- Reaction has significant effects on the temperature profile in the formation and wellbore temperature behavior. Reaction heat will form a temperature peak easy to identify since it is between cool acid temperature and geothermal temperature.
- The wellbore temperature behavior is sensitive to the acid injection rate, providing us a mechanism to determine the acid injection profile quantitatively. This also gives us confidence for future work.

5.2 Recommendations and Future Work

We have only single layer model in this research. However, the model should be developed for multilayer formation.

Besides, the inverse model should be developed to obtain the acid flow profile from the temperature data measured by DTS.

There are still some aspects of the model we can improve. For acid injection problem, we assume that the reaction only occurs at the front of wormholes. As a matter

of facts, many branches form with the main wormhole and reaction also happens at the branches. More accurate wormhole model may be used here.

In the flow-back problem, we neglected the heat conduction term in the energy balance equation because the heat convection is dominating. However, at the location of temperature peak, the temperature gradient is large, in other words, the heat conduction is important at this location.

In this research, the whole approach should include forward model and inverse model. Here we just developed part of the forward model which is a 1-D model. 2-D formation model can be developed with the consideration of the height of each layer.

Wellbore thermal model should be developed and coupled with the model we already had. The heat transfer in the wellbore will also affect the temperature behavior in the wellbore significantly.

NOMENCLATURE

Symbol		Description
C^0_{HCl}	=	concentration of HCl, weight fraction, dimensionless
C_{ps}	=	heat capacity of acid solution, m/Lt^{2}T, J/(kg·K)
C_{pR}	=	heat capacity of rock, m/Lt^{2}T , J/(kg·K)
e_k	=	specific kinetic energy of acid solution, m/Lt^2, J/kg
e_p	=	specific potential energy of acid solution, m/Lt^2, J/kg
e_R	=	specific internal energy of rock, m/Lt^2, J/kg
e_s	=	specific internal of acid solution, m/Lt^2, J/kg
E_{accu}	=	energy accumulating in the element, m^2/Lt^2, J
$E_{created}$	=	energy created in the element, m^2/Lt^2, J
E_{in}	=	energy flowing into the element, m^2/Lt^2, J
E_{out}	=	energy flowing out of the element, m^2/Lt^2, J
h	=	height of the layer, L, m [ft]
H	=	enthalpy of substance, L^{2}T^2, J/mol [kcal/mol]
$\hat{H}$	=	specific enthalpy of acid solution, m/Lt^2, J/kg
m	=	counter of grid block, dimensionless
M_R	=	molecular mass of rock, kg/mol
n_{HClcon}	=	mole of consumed HCl, mol
N_{AC}	=	acid capacity number, dimensionless
p	=	counter of time step, dimensionless

P = pressure, m/Lt^2, Pa

PV_{bt} = break through pore volumes, dimensionless

PV_{btopt} = optimum break through pore volumes, dimensionless

q = injection rate of acid solution, L^3/t, m^3/s [bbl/min]

q'' = heat flux caused by heat conduction, m/t^3, W/m^2

Q = volume of injected acid, L^3, m^3 [bbl]

Q_{reac} = reaction heat released by unit mole HCl, m^2/Lt^2, J/(molHCl)

r = radius, L, m

r_w = wellbore radius, L, m [ft]

R_s = radius of spent acid front, L, m

R_{wh} = radius of wormhole front, L, m

t = time, t, s

t_f = total flow back time, t, s

t_i = total injection time, t, s

T = temperature, T, K

T_a = temperature of acid injected, T, K

T_g = geothermal temperature, T, K

T_i = initial temperature of reservoir, T, K

u = velocity of acid solution, L/t, m/s

u_w = velocity of acid solution at wellbore radius, L/t, m/s

v = specific volume, L^3/m, m^3/kg

V_{dis} = volume of dissolved rock, L^3, m^3

V_F^0 = volumetric fraction of fast-reacting rock, dimensionless

V_i = interstitial velocity, L/t, m/s [cm/min]

V_{iopt} = optimum interstitial velocity, L/t, m/s [cm/min]

V_{wh} = velocity of wormhole growth, L/t, m/s [cm/min]

W_B = constant in wormhole model, $(L/t)^{-2}$, $(m/s)^{-2}$

W_{eff} = constant in wormhole model, $(L/t)^{1/3}$, $(m/s)^{1/3}$

W_t = time delay constant, t, s

z = coordinate in height direction of the layer, L, m

Greek

β_F = dissolve power of acid, weight fraction, dimensionless

η = wormhole efficiency, volumetric fraction, dimensionless

λ = heat conductivity of acid solution and rock, mL/t^3T, W/(m·K)

ρ_R = density of rock, m/L^3, kg/m^3

ρ_s = density of acid solution, m/L^3, kg/m^3

ϕ = porosity, volumetric fraction, dimensionless

ϕ_i = initial porosity, volumetric fraction, dimensionless

Δ = prefix for difference

Subscript

a = acid

con = consumed

dis = dissolved

F = fast reaction

i	=	initial
opt	=	optimum
R	=	rock
s	=	acid solution
w	=	well
wh	=	wormhole

REFERENCES

Buijse, M. and Glasbergen, G.: "A Semiempirical Model to Calculate Wormhole Growth in Carbonate Acidizing," paper SPE 96892 presented at the 2005 SPE Annual Technical Conference and Exhibition, Dallas, Texas, 9-12 October.

Clanton, R.W., Haney, J.A., Pruett, R., Wahl, C.L., Goiffon, J.J. and Gualtieri, D.: "Real-Time Monitoring of Acid Stimulation Using a Fiber-Optic DTS System," paper SPE 100617 presented at the 2006 SPE Western Regional/AAPG Pacific Section/GSA Cordilleran Section Joint Meeting, Anchorage, Alaska, 8-10 May.

Economides, M.J., Hill, A.D. and Ehlig-Economides, C.: *Petroleum Production System*, 400. 1993. Upper Saddle River, New Jersey: Prentice Hall, Inc.

Gao, G. and Jalali, Y.: "Interpretation of Distributed Temperature Data during Injection Period in Horizontal Wells," paper SPE 96260 presented at the 2005 SPE Annual Technical Conference and Exhibition, Dallas, Texas, 9-12 October.

Glasbergen, G., Gualtieri, D., Domelen, M.V. and Sierra, J.: "Real-Time Fluid Distribution Determination in Matrix Treatments Using DTS," paper SPE 107775 presented at the 2007 European Formation Damage Conference, Scheveningen, The Netherlands, 30 May- 1 June.

Johnson, D., Sierra, J., Kaura, J., and Gualtieri, D.: "Successful Flow Profiling of Gas Wells Using Distributed Temperature Sensing Data," paper SPE 103097 presented at the 2006 SPE Annual Technical Conference and Exhibition, San Antonio, Texas, 24-27 September.

Medeiros, F. and Trevisan, O.V.: "Thermal Analysis in Matrix Acidization," *Journal of Petroleum Science and Engineering*, 2006. **51**: 85-96.

Perry, R.H., Green, D.W. and Maloney, J.O: *Perry's Chemical Engineers' Handbook,* 226-231. 1963. New York: McGraw-Hill Book Co.

Wang, X., Lee, J., Thigpen, B., Vachon, G., Poland, S. and Norton, D.: "Modeling Flow Profile using Distributed Temperature Sensor (DTS) System," paper SPE 111790 presented at the 2008 SPE Intelligent Energy Conference and Exhibition, Amsterdam, The Netherlands, 25-27 February.

Whitson, C.H. and Kuntadi, A.: "Khuff Gas Condensate Development," paper SPE 10692 presented at the 2005 International Petroleum Technology Conference, Doha, Qatar, 21-23 November.

Yoshioka, K., Zhu, D., and Hill, A.D.: "A New Inversion Method to Interpret Flow Profiles from Distributed Temperature and Pressure Measurements in Horizontal

Wells," paper SPE 109749 presented at the 2007 SPE Annual Technical Conference and Exhibition, Anaheim, California, 11-14 November.

VITA

Name:	Xuehao Tan
Address:	Lifeng 5#, Zhanqian District Yingkou, Liaoning, 115000, China
Email Address:	xuehao.tan@pe.tamu.edu
Education:	B.E., Engineering Thermal Physics, Tsinghua University, 2007 M.S. Petroleum Engineering, Texas A&M University, 2009

This thesis was typed by the author.